'This is the peer reviewed version of the following article: Adrian D. Werner, Correction factor to account for dispersion in sharp-interface models of terrestrial freshwater lenses and active seawater intrusion, Advances in Water Resources, Volume 102, April 2017, Pages 45-52, ISSN 0309-1708,

which has been published in final form at
http://dx.doi.org/10.1016/j.advwatres.2017.02.001

Correction factor to account for dispersion in sharp-interface models of terrestrial freshwater lenses and active seawater intrusion

Adrian D. Werner[1,2*]

[1]School of the Environment, Flinders University, GPO Box 2100, Adelaide, SA 5001, Australia.

[2]National Centre for Groundwater Research and Training, Flinders University, GPO Box 2100, Adelaide, SA 5001, Australia.

*Corresponding author

Email address: Adrian D. Werner: adrian.werner@flinders.edu.au

Originally submitted to *Advances in Water Resources* on 1st October 2016

Abstract

In this paper, a recent analytical solution that describes the steady-state extent of freshwater lenses adjacent to gaining rivers in saline aquifers is improved by applying an empirical correction for dispersive effects. Coastal aquifers experiencing active seawater intrusion (i.e., seawater is flowing inland) are presented as an analogous situation to the terrestrial freshwater lens problem, although the inland boundary in the coastal aquifer situation must represent both a source of freshwater and an outlet of saline groundwater. This condition corresponds to the freshwater river in the terrestrial case. The empirical correction developed in this research applies to situations of flowing saltwater and static freshwater lenses, although freshwater recirculation within the lens is a prominent consequence of dispersive effects, just as seawater recirculates within the stable wedges of coastal aquifers. The correction is a modification of a previous dispersive correction for Ghyben-Herzberg approximations of seawater intrusion (i.e., stable seawater wedges). Comparison between the sharp interface from the modified analytical solution and the 50% saltwater concentration from numerical modelling, using a range of parameter combinations, demonstrates the applicability of both the original analytical solution and its corrected form. The dispersive correction allows for a prediction of the depth to the middle of the mixing zone within about 0.3 m of numerically derived values, at least on average for the cases considered here. It is demonstrated that the uncorrected form of the analytical solution should be used to calculate saltwater flow rates, which closely match those obtained through numerical simulation. Thus, a combination of the unmodified and corrected analytical solutions should be utilized to explore both the lens extent and the saltwater fluxes, depending on the dispersiveness of the problem. The new method developed in this paper is simple to apply and offers a wider range of application relative to the previous sharp-interface freshwater lens solution.

Introduction

Until recently, river-fed freshwater lenses in otherwise saline aquifers were presumed to occur under losing river conditions or require occasional influxes from floodwaters to persist during periods of low river flow. The occurrence of stable freshwater lenses adjacent to the river seems prima facie implausible if saline groundwater flows towards the river (i.e., the river is generally gaining). However, Werner and Laattoe (2016) showed using sharp-interface theory that buoyancy forces allow a stable freshwater lens to persist under steady-state conditions in regions where the river is gaining, demonstrating for the first time the plausibility, albeit theoretically, of terrestrial freshwater lenses near gaining rivers. Physical sand-tank experiments by Werner et al. (2016) validated Werner and Laattoe's (2016) discovery, and provided direct observations of freshwater lenses within gaining river conditions, although only under controlled laboratory-scale conditions. Their physical experimentation produced freshwater-saltwater mixing zones that were narrow, commensurate with the sharp-interface assumption of the analytical solution. Werner et al. (2016) showed that the prediction of near-river freshwater lenses requires direct observations of the lens to calibrate the analytical solution, given the uncertainties in aquifer parameters used to estimate the lens extent.

These terrestrial forms of the freshwater lenses commonly encountered in islands are found in the floodplain aquifers of semi-arid to arid settings, where saltwater may be found flowing towards otherwise freshwater rivers. For example, it is thought that the floodplains of the River Murray host stable freshwater lenses despite gaining river conditions (e.g., Viezzoli et al., 2009). The River Murray is highly regulated, with the river almost a continuous sequences of locks and weirs. Aside from periods of floods, the river is not as dynamic as an unmodified river. River Murray freshwater lenses are critically important for the health of threatened ecosystems, and provide other positive functions within otherwise semi-arid and arid riparian settings (e.g., Woods, 2015). Despite this, their prevalence and extent have not been measured through detailed and targeted field monitoring programs, and only approximate dimensions (e.g., some few 100s of meters in length and depths of up to 15 m; Viezzoli et al., 2009) are ascertainable from a limited number of field investigations employing geophysical methods.

The key distinction between terrestrial freshwater lenses near gaining rivers and those of islands is that on islands, the freshwater flows towards the sea while the underlying seawater is relatively static (e.g., Post et al., 2013), whereas saltwater flows towards the river beneath comparatively immobile freshwater in the terrestrial case (e.g., Werner et al., 2016). These conditions are assumed to apply at least to narrow mixing zone conditions. The conceptual model for terrestrial freshwater lenses is illustrated in Figure 1, which shows a fully penetrating river in a saline aquifer, with riverbed material of thickness B_r. The riverbed layer is intended to represent low-permeability material commonly found in the beds of slow-flowing rivers, e.g. due to colmation. The lens watertable matches the river water level due to the lack of flow within the lens, as discussed by Werner and Laattoe (2016). Note that the origin of x in Figure 1 lies to the left of the riverbed as shown by Werner et al. (2016), which corrects the corresponding diagram of Werner and Laattoe (2016). Other variables are explained in the following section.

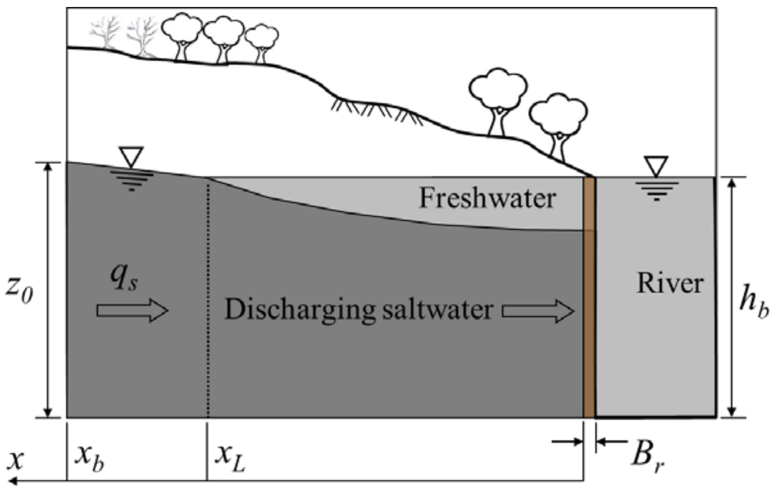

Figure 1. Terrestrial freshwater lens conceptual model. Light grey and dark grey are freshwater and saltwater, respectively.

The riparian freshwater lens conceptualization illustrated in Figure 1 can also be applied to a particular type of active seawater intrusion in coastal aquifers. Active seawater intrusion involves a groundwater hydraulic gradient that slopes downwards in the inland direction (i.e., freshwater discharge to the sea ceases), thereby causing seawater to advance inland under both advective and density-driven forces (Badaruddin et al., 2015; Werner, 2016). This is in contrast to the more commonly studied problem of passive seawater intrusion, which involves seawater underlying fresh groundwater flowing towards the coastline (e.g., Strack, 1976; Werner et al., 2012). In the case of active seawater intrusion, the left boundary of Figure 1 represents the sea, while the right boundary represents a location inland where freshwater can be found. Hereafter, the left and right boundaries of Figure 1 are referred to simply as the saltwater and freshwater boundaries, respectively.

Application of the analytical solution of Werner and Laattoe (2016) to active seawater intrusion requires a freshwater boundary condition that removes saline groundwater while maintaining a source of freshwater for the lens. Such an arrangement might conceivably occur where drainage systems have been installed in coastal settings to remove saltwater, although the drains need to maintain a low salinity, and as such would require continuous flushing with freshwater from elsewhere. Some of the freshwater lenses underlying Dutch polders (e.g., Velstra et al., 2011) may match this conceptual model. The active seawater intrusion analogue also requires equilibrium conditions, in which the inland flow of seawater is removed at the freshwater boundary. These two conditions are an unlikely combination in aquifers where active seawater intrusion is created by freshwater pumping, because pumping is likely to cease once seawater reaches the well. However, if the inland boundary is a body of surface water (e.g., wetland, canal or drain), the flowing seawater may be discharged to an otherwise freshwater boundary where saltwater is continuously flushed from the surface feature. The inland boundary salinity must remain fresh for the analytical solution to apply, because it serves as a source of recirculation within the lens, at least in the presence of dispersive effects. In any case, situations of terrestrial freshwater lenses are themselves important enough to pursue the aims of the current research.

Whether it is applied to terrestrial freshwater lenses or active seawater intrusion, a significant limitation of the analytical method of Werner and Laattoe (2016) is the sharp-interface assumption. In coastal aquifers, this is known to lead to over-estimation of the extent of seawater in the coastal aquifer (Volker and Rushton, 1982). Given that Werner and Laattoe (2016) reverse the coastal aquifer scenario of flowing freshwater-stagnant seawater in their riverine setting, it is likely that the sharp-interface assumption over-estimates the extent of the freshwater lens. A recent numerical modelling investigation of seawater intrusion by Werner (2016) demonstrates this effect, whereby the addition of dispersion to active seawater intrusion simulations creates a significantly reduced freshwater lens, both during transient development and under the final steady-state conditions. Where dispersion is significant, as is more often the case in real-world settings involving freshwater-saltwater mixing (e.g., Lu et al., 2009; Cartwright et al., 2010; Werner et al., 2013), the Werner and Laattoe (2016) analytical solution is inapplicable.

An empirical correction to sharp-interface methods to account for dispersion in the estimation of stable seawater wedges in coastal aquifers was proposed by Pool and Carrera (2011), and subsequently modified by Lu and Werner (2013). The method applies to the classic condition of flowing freshwater and stable seawater. The current paper aims to devise an analogous empirical correction to that developed by Pool and Carrera (2011) for application to the Werner and Laattoe (2016) analytic solution. Numerical modelling experiments test the applicability and robustness of the correction, in terms of the lens extent and saltwater and freshwater fluxes, under various dispersive and advective conditions. It is expected that the new correction will allow for improved estimation of freshwater lens extents within both terrestrial (i.e., riparian) settings and coastal aquifers experiencing active seawater intrusion, whereby the over-estimation of freshwater lens size arising from the sharp-interface assumption is alleviated. The current method applies to steady-state conditions and is intended as only a first-estimate of freshwater lens extent, such that the influence of floodplain inundation, river level fluctuations, lens creation, and other transient processes require alternative techniques of analysis.

Correcting Werner and Laattoe’s (2016) solution for dispersion effects

Werner and Laattoe (2016) provide the following solution to steady saltwater flow towards a river containing freshwater (see Figure 1):

$$q_s = \frac{\left(z_0^2 - \dfrac{h_b^2}{(\delta+1)}\right)}{2\left(\dfrac{x_b}{K} + \dfrac{B_r}{K_r}\right)} \tag{1}$$

Here, q_s [L^2 T^{-1}] is saltwater flow, which is positive for flow towards the freshwater boundary, K [L T^{-1}] is homogeneous and isotropic hydraulic conductivity, and z_0 [L] is the water depth at the saltwater boundary, representing the depth of the aquifer base below sea level (coastal setting) or the depth of saltwater at some known location in the vicinity of a river (terrestrial setting). h_b [L] is the depth of water at the freshwater boundary, which is situated at x_b from the saltwater boundary, and δ is the dimensionless density difference $(\rho_s - \rho_f)/\rho_f$, where ρ_f and ρ_s [M L^{-3}] are freshwater and saltwater densities, respectively. K_r [L T^{-1}] and B_r [L] are the hydraulic conductivity and thickness of any riverbed material. In the absence of resistive material at the aquifer-ocean interface in coastal settings, K_r and B_r are taken as K and 1 m, respectively.

Simple manipulation of Werner and Laattoe's (2016) equations leads to a solution for the horizontal length (x_L) of the freshwater lens:

$$x_L = \frac{\dfrac{\delta}{\delta+1} x_b + \dfrac{KB_r}{K_r}\left(1 - \dfrac{z_0^2}{h_b^2}\right)}{\left(\dfrac{z_0^2}{h_b^2} - \dfrac{1}{\delta+1}\right)} \tag{2}$$

Werner and Laattoe's (2016) theory provides the basis for determining the freshwater-saltwater interface, as:

$$\eta_s = \sqrt{\frac{\left(z_0^2 - \frac{h_b^2}{(\delta+1)}\right)\left(\frac{\delta+1}{\delta}\right)\left(\frac{KB_r}{K_r} + x\right)}{\left(x_b + \frac{KB_r}{K_r}\right)}} \quad (3)$$

Here, η_s [L] is the height of the freshwater-saltwater interface above the aquifer basement and x [L] is the distance from the freshwater boundary.

The approach to correcting the above equations to account for dispersion is founded on the strategy of Pool and Carrera (2011), who provided a correction for immobile rather than flowing seawater. Their method adjusts sharp-interface solutions (based on the Ghyben-Herzberg condition) by changing the dimensionless density, thereby improving the match between analytical predictions and dispersive numerical modelling of the freshwater-saltwater mixing zone. Lu and Werner (2013) adopted a modified form of the Pool and Carrera (2011) correction formula to apply to cross-sectional conceptual models similar to those of the current study, as:

$$\delta^* = \delta\left[1 - \left(\frac{\alpha_T}{z_0}\right)^{1/4}\right] \quad (4)$$

Here, δ^* is the corrected value of δ, and α_T [L] is transverse dispersivity. Pool and Carrera (2011) used 1/6 rather than 1/4 as the exponent in equation (4).

Equation (4) and Pool and Carrera's (2011) original formulation have proven effective in correcting for the over-estimation in seawater extent from sharp-interface methods (e.g., Lu et al., 2012; Lu and Werner, 2013; Werner, 2016), at least for stable bodies of motionless seawater. The basis for equation (4) is the premise that the density force that drives seawater inland needs to be reduced, thereby resulting in a smaller body of seawater in the coastal aquifer, commensurate with dispersive model estimates. The sharp-interface over-estimation of stable seawater wedges is attributable to the elimination of seawater recirculation in sharp-interface assumptions, whereby dispersion is neglected (Abarca et al., 2007; Post et al., 2013). That is, the sharp-interface assumption neglects the head losses in the seawater wedge that accompany dispersion-driven recirculation, leading to artificially larger seawater extents (Pool et al., 2011).

In the case of a stable freshwater lens overlying moving saltwater (Figure 1), the sharp-interface approach is expected to lead to over-estimation of the body of freshwater, rather than the saltwater extent. That is, under the assumption of sharp-interface conditions, the head losses due to freshwater lens recirculation are neglected, and the lens' driving force is thereby over-estimated. Pool and Carrera's (2011) method applied to Werner and Laattoe's (2016) analytical solution translates to a reduction in the buoyancy force that drives the freshwater lens away from the river. This can be effected by increasing the saltwater density or reducing the freshwater density. Regardless, according to Pool and Carrera's (2011) method, δ is lowered to δ^* and substituted into the respective solution to the sharp-interface distribution.

Initial attempts to adjust equations (1) to (3) by direct substitution of δ^* for δ resulted in a poor match between the modified analytical solution and corresponding numerical simulations, regardless of the values adopted for the equation (4) exponent, or for α_T and z_0. The problem with applying Pool and Carrera's (2011) correction in its original form is demonstrated by the following thought-experiment, and considering equations (2) and (3). The freshwater lens of Werner and Laattoe (2016) has a horizontal watertable, commensurate with the lack of surface recharge and the lens immobility. Thus, at x_L, the thickness of saltwater (η_s) will equal the aquifer thickness at the freshwater boundary (h_b), which in turn equals z_0 if the saltwater boundary is placed conveniently at x_L. Substituting this condition into equations (2) or (3) eliminates δ from the solution to x_L or η_s, at least when the boundary condition is specified at the limit of the lens (i.e., if $x_L = x_b$ is chosen for the purposes of demonstrating the point). Therefore, substituting δ for δ^* fails to modify the solution, and Pool and Carrera's (2011) approach becomes redundant. Hence, an alternative strategy is required, notwithstanding that changing the buoyancy force remains the most likely method to successfully correct the sharp-interface analytical solution for dispersion effects.

A novel modification to modifying Pool and Carrera's (2011) approach is adopted here whereby the buoyancy correction is applied as a change to the freshwater boundary water level, rather than direct modification of dimensionless density. The new freshwater boundary head is obtained by enforcing pressure equilibrium at the base of the river, which leads to:

$$h_b^* = \frac{\delta^* + 1}{\delta + 1} h_b \tag{5}$$

Equation (5) recognizes that the driving force for the lens is the height of the freshwater boundary water level, whereas changes to freshwater or saltwater density, as per Pool and Carrera's (2011) method, merely serve to modify saltwater discharge by changing the saltwater hydraulic gradient between the boundaries, as shown in the above thought experiment.

Substitution of equation (4) into equation (5) produces a new correction factor formula applicable to the Werner and Laattoe (2016) analytical solution, as:

$$h_b^* = \frac{\delta\left[1-\left(\frac{\alpha_T}{z_0}\right)^{1/4}\right]+1}{\delta+1}h_b \qquad (6)$$

The validity of Equation (6) is explored through numerical experimentation, as described in the section that follows.

Comparison to numerical modelling

Description of model setup

The numerical modelling of Werner (2016), who used SEAWAT (Langevin et al., 2008) to explore threshold parameter combinations that lead to different classes of seawater intrusion, is extended to evaluate the proposed correction, given as equation (6). Various parameter combinations and aquifer geometries are tested using cross-sectional simulations of a shallow unconfined coastal aquifer devoid of distributed recharge.

The base case numerical model adopts the same grid as Werner (2016), comprising a relatively fine resolution (0.05 m by 0.05 m near the sea boundary, increasing to 10 m by 0.05 m at the inland boundary). Computational effort is offset by the modest domain size (i.e., 5.2 m deep by 200 m long). This model setup was shown by Werner (2016) to limit artificial numerical dispersion. The domain size and mesh resolution were modified to simulate alternative aquifer geometries, but in all cases, the same number of model cells (124,800) was used to yield reasonable model run times (up to three days for some simulations). Decreasing the domain size, which creates steeper head gradients for a given head difference between the freshwater and saltwater boundaries, allowed for a finer grid resolution near the right-hand side of the model. The maximum cell size was reduced from 10 m in the base case to 0.55 m in simulations with the adoption of the smallest domains.

Models grids were evaluated by comparing non-dispersive numerical simulations with the original analytical solution of Werner and Laattoe (2016). Figure 2 illustrates the model boundary conditions and geometry, as adopted by Werner (2016) and representing the base case simulation in the current paper.

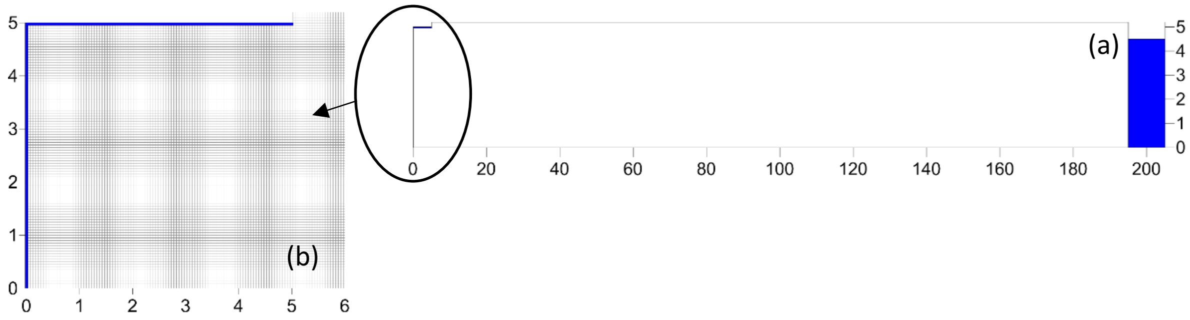

Figure 2. Base case numerical model layout: (a) model domain, and (b) close-up of the left boundary showing the model grid. Blue cells represent specified head and concentration boundary conditions, whereby solute leaves the model at the ambient concentration, but enters the model from the left (saltwater boundary; solute concentration = 1) as saltwater and from the right (freshwater boundary; solute concentration = 0) as freshwater. Units are meters.

The parameters of the base case model were chosen based on experience and are considered reasonable for River Murray conditions (i.e., consistent with parameter ranges provided by Werner and Laattoe (2016) for typical River Murray conditions), and for coastal aquifers in general. Values are given in Table 1, which also lists parameter ranges associated with additional simulations intended to explore a wider variety of conditions. The base case corresponds to Case 3_d in Werner (2016).

Table 1. Parameters adopted in numerical and analytical models.

Parameter	Symbol	Base case value	Tested range	Unit
Onshore aquifer length	x_b	195	95 to 395	m
Offshore aquifer length		5	-	m
Aquifer base below sea level	z_0	5	10 to 30	m
Inland boundary head	h_b	4.99	z_0 – 0.1 to z_0	m
Isotropic hydraulic conductivity	K	10	1 to 100	m/d
Specific yield	S_y	0.24	-	-
Specific storage	S_s	10^{-5}	-	1/m
Effective porosity	n	0.3	-	-
Longitudinal dispersivity	α_L	1	0 to 10	m
Transverse dispersivity	α_T	$\alpha_L/10$	0.01 to 1	m
Molecular diffusion	D_m	8.64×10^{-5}	0	m^2/d
Freshwater density	ρ_f	1000	-	kg/m^3
Saltwater density	ρ_s	1025	1010 to 1040	kg/m^3

Evaluating the correction term: Salinity distributions

The steady-state salinity distributions of numerical models and the sharp interface of the analytical solution (i.e., corrected for dispersion in dispersive cases and uncorrected in non-dispersive cases) are included in Figure 3. Twenty cases were used to represent the range of parameters given in Table 1. A description of each case is provided in Table 2, which also lists the discrepancy between the analytical approach and the 0.1 and 0.5 relative salinity contours (i.e., 10% and 50% saltwater concentrations) from numerical models.

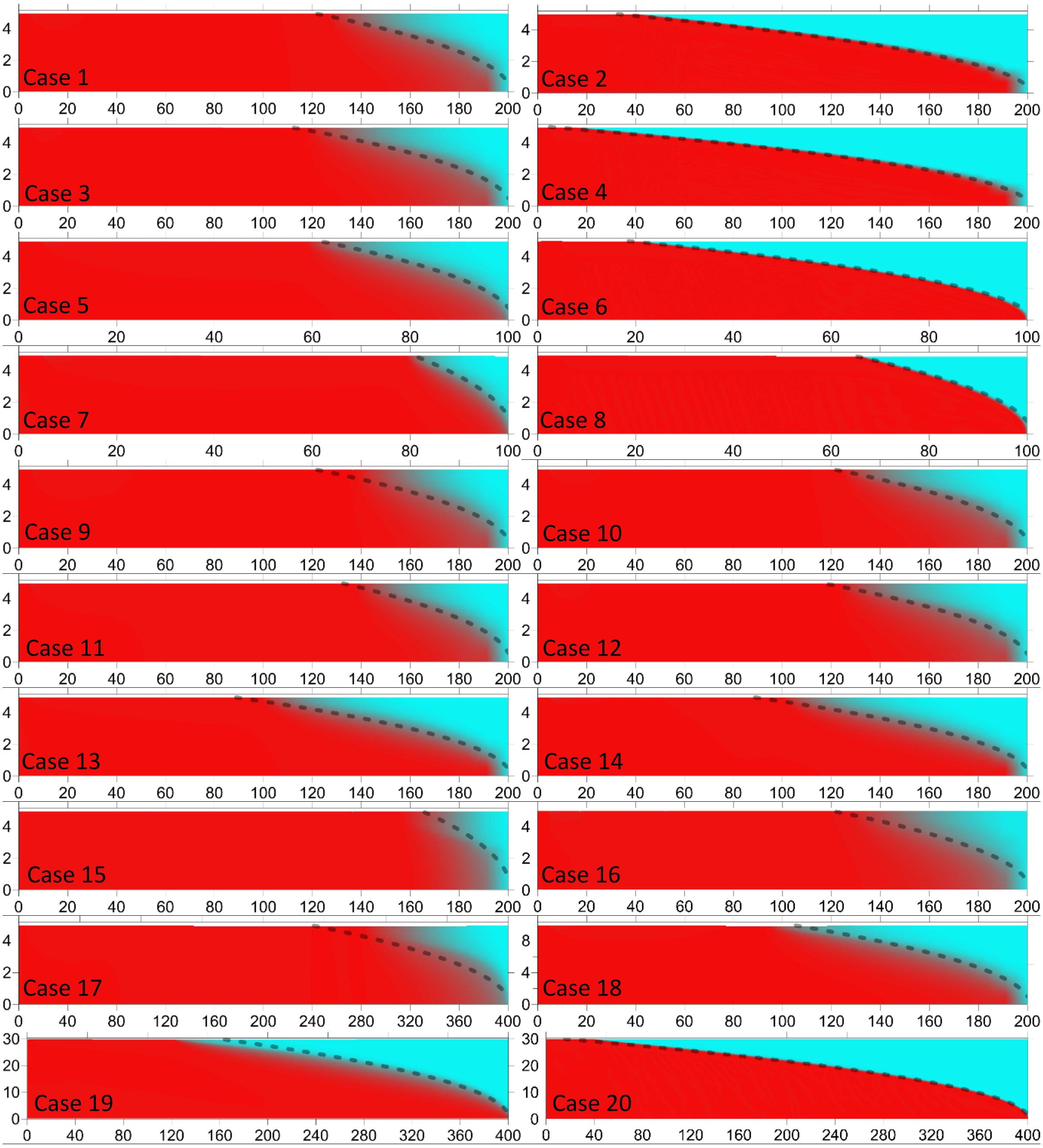

Figure 3. Comparison between numerical model salinity distributions (colors; blue is freshwater and red is saltwater) and sharp-interface locations (dotted line) from analytical solution (corrected for dispersive cases and uncorrected for non-dispersive cases). Note vertical and horizontal scale differences between cases. An explanation of each case is given in Table 2. Units are meters, and salinity ranges from 0 (freshwater) to 1 (saltwater).

Table 2. Sensitivity cases. Parameters correspond to those used in the base case unless stated otherwise. The average error (average of discrepancies at model cell centers) is positive where the specified isochlor from the numerical model is higher in elevation than the analytical sharp interface. Average error values arising from the uncorrected analytical solution are given in brackets for dispersive simulations. “N/A” infers that all concentrations were higher than 0.1.

Case	Variation from base case	Average error in interface elevation (m)	
		0.1 isochlor	0.5 isochlor
1	None	1.2 (1.9)	0.17 (1.2)
2	$\alpha_L = \alpha_T = 0$, $D_m = 0$	0.14	0.09
3	$h_b = 5$ m	1.2 (1.9)	0.16 (1.2)
4	$h_b = 5$ m, $\alpha_L = \alpha_T = 0$, $D_m = 0$	0.13	0.08
5	$x_b = 95$	0.95 (1.7)	-0.15 (0.8)
6	$x_b = 95$, $\alpha_L = \alpha_T = 0$, $D_m = 0$	0.05	0.001
7	$x_b = 95$, $h_b = 4.9$ m	0.81 (1.5)	-0.28 (0.6)
8	$x_b = 95$, $h_b = 4.9$ m, $\alpha_L = \alpha_T = 0$, $D_m = 0$	0.03	-0.06
9	$K = 1$ m/d	1.5 (2.1)	0.27 (1.1)
10	$K = 100$ m/d	1.1 (1.8)	0.15 (1.2)
11	$\rho_s = 1010$ kg/m^3	1.4 (2.1)	0.11 (1.0)
12	$\rho_s = 1040$ kg/m^3	1.2 (1.8)	0.14 (1.1)
13	$\alpha_L = 0.1$ m, $\alpha_T = 0.01$ m	0.83 (1.3)	0.11 (0.7)
14	$\alpha_L = 1$ m, $\alpha_T = 0.01$ m	0.93 (1.4)	0.12 (0.7)
15	$\alpha_L = 1$ m, $\alpha_T = 1$ m	N/A (N/A)	-0.30 (1.5)
16	$\alpha_L = 10$ m, $\alpha_T = 0.1$ m	N/A (N/A)	0.04 (0.9)
17	$x_b = 395$	1.5 (2.0)	0.44 (1.2)
18	$z_0 = 10$ m	1.1 (2.6)	-0.34 (1.7)
19	$x_b = 395$, $z_0 = 30$ m	0.78 (4.9)	-1.6 (2.9)
20	$x_b = 395$, $z_0 = 30$ m, $\alpha_L = \alpha_T = 0$, $D_m = 0$	0.63	0.31

The results given in Figure 3 and Table 2 highlight the applicability of the analytical solution of Werner and Laattoe (2016) for narrow mixing zone conditions. For example, on average, the sharp interface from the uncorrected analytical solution is only 0.11 m lower than the 0.5 salinity isochlor from non-dispersive numerical simulations (Cases 2, 4, 6, 8 and 20). This over-estimation of the 0.5 isochlor is attributable mainly to the minor amount of unavoidable artificial dispersion in SEAWAT, which produces slightly smaller lenses than would otherwise occur in completely non-dispersive conditions. Artificial dispersion was assessed by obtaining the value of α_T that, when adopted in the corrected analytical solution, reproduced the non-dispersive results of SEAWAT. The calibrated value of α_T optimized the discrepancy between the corrected analytical solution and non-dispersive numerical modelling, whereby larger values of α_T indicate more artificial dispersion. This produced an optimal α_T value of 1.9×10^{-6} m, which roughly halved the mismatch between the sharp interface and 0.5 isochlor in non-dispersive results, i.e., from 0.11 m (α_T = 0) to 0.054 m (α_T = 1.9×10^{-6} m). This supports the accuracy of the SEAWAT model setup and verifies the low artificial numerical dispersion within non-dispersive simulations.

The largest analytical solution-numerical model mismatch in non-dispersive results was obtained for Case 20, which involved the longest and deepest model domain. Given that all models have the same number of cells, this model also involved the largest cell sizes, on average. The optimization of α_T described above served to reduce the error of 0.31 m for Case 20 (see Table 2) to 0.00 m. Thus, it appears that the effects of artificial numerical dispersion were strongest in this case, most likely as a consequence of the larger cell size.

Paired simulations with and without dispersion (Cases 1 and 2, Cases 3 and 4, Cases 5 and 6, Cases 19 and 20) show that smaller lenses occur under dispersive conditions. This is expected given the earlier explanation regarding dispersive effects on seawater wedge extents in coastal settings. Figure 3 and Table 2 verify that the proposed correction factor successfully extends the analytical solution to dispersive conditions. The dispersive correction reduced the mismatch between the analytically derived sharp interface and the 50% salinity contour by around an order of magnitude in dispersive simulations (Table 2). Errors in predicting the 50% salinity using the corrected analytical solution were 11% of the lens thickness for dispersive simulations, and were 8.5% for non-dispersive simulations estimated by the uncorrected analytical solution. This means that the corrected analytical solution is almost as proficient at predicting the dispersive interface as the uncorrected analytical solution is able to predict the non-dispersive interface.

Both positive and negative mismatches between the 0.5 salinity contour of dispersive simulations and the sharp interface from the corrected analytical solution are evident in Table 2. Thus, there is not an especially strong bias in the mismatch. A general observation from Figure 3 is that the corrected analytical solution matches the interface especially well in the middle parts of the lens, and tends to over-estimate the location of the lens tip, which has a somewhat truncated shape in the dispersive modelling results. On average, the corrected analytical solution produced interface elevations that were higher than the 0.5 salinity contour by 0.06 m, while the average absolute discrepancy between numerical and analytical approaches was 0.29 m. The largest mismatch between the 0.5 salinity contour and the sharp interface was -1.56 m, which arose from the results for the deepest and longest aquifer (Case 19). For this case, the corrected analytical solution matches better with the 0.1 isochlor from numerical modelling.

The complex interplay between longitudinal and transverse dispersivity in different parts of the model domain makes it challenging to attribute particular aspects of the analytical-numerical mismatch to clear causes. Where the interface is perpendicular to the flow direction (e.g., at the lens tip), it is likely that α_L, being ten times that of α_T in the majority of simulations, causes the lens to truncate under the enhanced dispersive mixing. This is particularly apparent in the lens shape of Case 16, where α_L is increased by an order magnitude relative to other cases and relative to α_T.

The exponent of 1/4 used in the dispersive correction given as equation (6) was assessed using calibration, noting that Lu and Werner (2013) and Pool and Carrera (2013) obtained different values through calibration. Optimization of the exponent was undertaken to ideally match the corrected analytical solution to the 0.5 isochlor, and a calibrated exponent of 0.28 was derived. This is slightly higher than the Lu and Werner (2013) value of 0.25 in equation (6). The value of 0.28 lowered the analytical-numerical discrepancy of Case 19 significantly, i.e., from -1.56 m to -0.71 m, and the average absolute error displayed a modest reduction from 0.29 m to 0.27 m.

Evaluating the correction term: Freshwater-saltwater flow patterns

The applicability of the dispersive correction to the Werner and Laattoe (2016) formula is founded on the expectation that dispersion drives freshwater recirculation within the lens. The slight over-estimation of lens extent in non-dispersive simulations indicates that some recirculation occurred in those cases, as mentioned above. Advective groundwater flowlines extracted from the SEAWAT results are provided in Figure 4 to demonstrate recirculation patterns in Case 1 (dispersive) and Case 2 (non-dispersive).

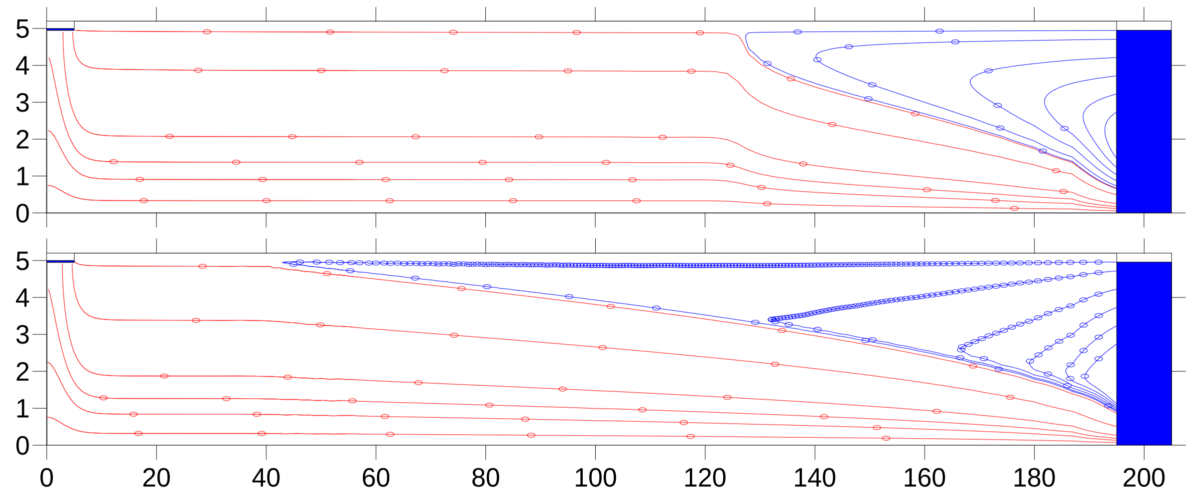

Figure 4. Advective path lines for Cases 1 and 2 are shown in the upper and lower sub-figures, respectively. Units are meters. Red and blue lines originally enter the aquifer as saltwater (from the left) and freshwater (from the right), respectively. Freshwater circulation is counterclockwise. Circles on the flow lines are located at 5-yearly intervals.

The recirculation patterns in Figure 4 show marked differences between dispersive (Case 1) and non-dispersive (Case 2) conditions, such as the rounded versus angular patterns of advective particle movement. In the dispersive case, the oldest freshwater recirculated for some 26 years, whereas the maximum residence time of freshwater increased to about 900 years when dispersion parameters were set to zero. Post et al. (2013) found that saltwater recirculated in their coastal aquifer setting for 100s up to 20,000 years, and Chesnaux and Allen (2008) obtained island freshwater lens residence times of 10s to 1000s of years for travel distances of 100’s of meters; similar to the scale of the conceptual models adopted here. Hence, the current residence times are within the range of reported values, albeit the variability of previous studies is wide. The saltwater residence times of dispersive cases are longer than non-dispersive cases by approximately 5 years.

Despite significant differences in salinity distributions between paired dispersive and non-dispersive simulations, the saltwater fluxes were otherwise very similar. This is evident in the flux values provided in Table 3, which reports saltwater fluxes at the downstream boundary from both the analytical and numerical approaches, and provides freshwater recirculation rates from the numerical model (freshwater flow in the analytical approach is zero).

Table 3. Analytical and numerical saltwater outflow rates (m^3/d) at the downstream (freshwater) boundary, and freshwater recirculation rates (m^3/d) from the numerical model. "N/A" identifies non-dispersive cases, for which the dispersive correction to the analytical solution was not required.

Case	Saltwater outflow			Freshwater inflow/outflow
	Numerical model	Original Analytical solution	Modified Analytical solution	Numerical model
1	0.0184	0.0180	0.0237	0.0132
2	0.0184	0.0180	N/A	0.0020
3	0.0157	0.0156	0.0213	0.0129
4	0.0159	0.0156	N/A	0.0017
5	0.0374	0.0368	0.0484	0.0436
6	0.0374	0.0368	N/A	0.0043
7	0.0828	0.0821	0.0933	0.0525
8	0.0832	0.0821	N/A	0.0081
9	0.0018	0.0018	0.0024	0.0015
10	0.1827	0.1804	0.2373	0.1304
11	0.0088	0.0088	0.0112	0.0056
12	0.0276	0.0270	0.0358	0.0209
13	0.0184	0.0180	0.0212	0.0061
14	0.0183	0.0180	0.0212	0.0066
15	0.0184	0.0180	0.0281	0.0215
16	0.0184	0.0180	0.0237	0.0128
17	0.0091	0.0089	0.0117	0.0278
18	0.0683	0.0672	0.0864	0.0304
19	0.2893	0.2846	0.3495	0.1195
20	0.2893	0.2846	N/A	0.0211

Table 3 demonstrates that, as expected, saltwater flow rates are higher for larger values of K, δ, z_0 and head difference across the model, and for smaller distance between boundaries, in accordance with equations (1) to (3). Reducing dispersion parameters to zero in the numerical model caused a very small increase in saltwater flow rates, although this was undetectable in paired cases 19 and 20. Therefore, the shorter saltwater residence times of Case 2 (non-dispersive) relative to Case 1, as shown in Figure 4, are not primarily caused by differences in saltwater flow rates. Rather, the larger extent of the freshwater lens in the non-dispersive case reduces the cross-sectional area available for saltwater flow, thereby increasing the velocity and lowering the residence times relative to the dispersive case.

The most striking feature of the Table 3 results is that the correction term corrupts the saltwater flow rates, whereas the unmodified solution of Werner and Laattoe (2016) performs well in obtaining the saltwater flow rates of the numerical model. Thus, whereas the position of the mixing zone is best obtained using the correction term of equation (6), saltwater fluxes should be calculated without the correction and adopting the unmodified Werner and Laattoe (2016) formulae, given as equations (1) to (3). It remains to be assessed as to whether Pool and Carrera's (2011) correction, applied to the stable seawater wedges for which it was intended, also produces erroneous fluxes.

Freshwater recirculation rates are higher in dispersive cases relative to non-dispersive cases, as expected given the effects of dispersive freshwater entrainment in flowing saltwater. In most of the dispersive cases, freshwater fluxes are of similar order to saltwater fluxes, in contrast to the assumption of Werner and Laattoe's (2016) analytical solution of relatively immobile freshwater, which they adopt for narrow mixing zone situations. The non-dispersive cases in Table 3 produced small freshwater fluxes, thereby supporting their assumption.

Freshwater recirculation fluxes increase with larger values of K, δ, z_0 and head difference across the model, and for larger distance between boundaries. Smith (2004) observed complex relationships between aquifer parameters and seawater recirculation patterns in coastal aquifers, whereby the density-driven overturn broke down as z_0 and α_T approaches extreme (high or low) values. In his analysis, maximum rates of density-driven seawater circulation were achieved for large values of K_z and δ, in agreement with the freshwater lens observations of the current study. Further analysis is needed to assess whether freshwater recirculation follows the same trends as those observed for seawater in coastal aquifers by Smith (2004) for the full gamut of parameter combinations likely to be encountered in both terrestrial and coastal lens situations.

Conclusions

This research extends the Werner and Laattoe (2016) analytical solution for the steady-state extent of a freshwater lens overlying flowing saltwater so that it applies to dispersive situations, which are expected to be more common than the narrow mixing zone conditions for which their solution was developed. It achieves this by adapting the dispersive correction of Pool and Carrera (2011), applicable to coastal aquifers containing freshwater discharge to the sea, to the reversed situation of flowing saltwater and relatively stationary freshwater.

A new dispersive correction equation for modifying the freshwater boundary water level is devised to impose the buoyancy force reduction that is needed to reduce the size of the freshwater lens, such that the sharp-interface approximation is commensurate with the middle of the dispersive mixing zone predicted by a numerical approach. Testing of the new correction factor, applied to the Werner and Laattoe (2016) analytical solution, shows favorable matches to the results of dispersive numerical modelling for a range of parameters. The unmodified analytical solution is also an excellent match to several non-dispersive numerical modelling cases.

Calibration of the analytical solution was undertaken to examine the validity of the correction factor's exponent of 0.25, which was the value recommended by Lu and Werner (2013). Only a minor improvement in the match between analytical and numerical results could be obtained with an optimal exponent value of 0.28. Calibration of the transverse dispersivity (α_T) used in the correction factor equation was undertaken to seek an ideal match with non-dispersive numerical simulations, producing a small α_T of 1.9×10^{-6} m, demonstrating that the results of SEAWAT models contained low levels of artificial numerical dispersion.

Freshwater recirculation was found to be the primary process that leads to the effectiveness of the buoyancy modification via application of the correction factor. Flowlines obtained from two numerical modelling cases demonstrate the markedly stronger lens recirculation that arises when dispersion parameters are increased from zero to typical values (e.g., α_L = 1 m). Adding dispersion to numerical simulations also slowed saltwater velocities, leading to slightly longer saltwater residence times.

Saltwater fluxes predicted by the numerical model were well matched by the original analytical solution of Werner and Laattoe (2016) for both dispersive and non-dispersive cases, whereas the dispersive correction factor produced erroneous saltwater flow rates in dispersive situations. Thus, the unmodified analytical solution of Werner and Laattoe (2016) should be retained for estimates of saltwater fluxes, whereas the correction factor successfully reproduces the middle of dispersive mixing zones, to a reasonable level of accuracy.

Extensions to the current work are warranted to test a wider range of situations under which dispersive corrections to sharp-interface solutions may be used to positive effect. For example, it would be worthwhile to test whether the dispersive correction applies to models of transient interface movements, heterogeneous aquifers and systems receiving recharge, and incorporating other real-world processes that are neglected in the current analysis.

Acknowledgements

The author gratefully acknowledges the support of the Australian Research Council's Future Fellowship scheme (project number FT150100403). This research was partly supported under the Australian Research Council's Linkage Projects funding scheme (project number LP140100317). The constructive comments of three anonymous reviewers led to improvements to this article.

References

Abarca, E., J. Carrera, X. Sánchez-Vila, and M. Dentz (2007), Anisotropic dispersive Henry problem, Advances in Water Resources, 30, 913-926, doi: 10.1016/j.advwatres.2006.08.005.

Badaruddin, S., A. D. Werner and L. K. Morgan (2015), Water table salinization due to seawater intrusion, Water Resources Research, 51(10), 8397-8408, doi: 10.1002/2015WR017098.

Cartwright, I., T. R. Weaver, C. T. Simmons, L. K. Fifield, C. R. Lawrence, R. Chisari and S. Varley (2010), Physical hydrogeology and environmental isotopes to constrain the age, origins, and stability of a low-salinity groundwater lens formed by periodic river recharge: Murray Basin, Australia, Journal of Hydrology, 380, 203-221, doi: 10.1016/j.jhydrol.2009.11.001.

Chesnaux, R. and D. M. Allen (2008), Groundwater travel times for unconfined island aquifers bounded by freshwater or seawater, Hydrogeology Journal, 16, 437-445, doi: 10.1007/s10040-007-0241-6.

Langevin, C. D., D. T. Thorne, Jr., A. M. Dausman, M. C. Sukop and W. Guo (2008), SEAWAT Version 4: A Computer Program for Simulation of Multi-Species Solute and Heat Transport: U.S. Geological Survey Techniques and Methods Book 6, Chapter A22, 39 p., Reston.

Lu, C., Y. Chen and J. Luo (2012), Boundary condition effects on maximum groundwater withdrawal in coastal aquifers, Ground Water, 50(3), 386-393, doi: 10.1111/j.1745-6584.2011.00880.x.

Lu, C., P. K. Kitanidis and J. Luo (2009), Effects of kinetic mass transfer and transient flow conditions on widening mixing zones in coastal aquifers, Water Resources Research, 45, W12402, doi: 10.1029/2008WR007643.

Lu, C. and A. D. Werner (2013), Timescales of seawater intrusion and retreat, Advances in Water Resources, 59, 39-51, doi: 10.1016/j.advwatres.2013.05.005.

Pool, M. and J. Carrera (2011), A correction factor to account for mixing in Ghyben-Herzberg and critical pumping rate approximations of seawater intrusion in coastal aquifers, Water Resources Research, 47, W05506, doi: 10.1029/2010WR01025.

Pool, M., J. Carrera, M. Dentz, J. Hidalgo and E. Abarca (2011), Vertical average for modeling seawater intrusion, Water Resources Research, 47, W11506, doi: 10.1029/2011WR010447.

Post, V. E. A., A. Vandenbohede, A. D. Werner, Maimun and M. D. Teubner (2013), Groundwater ages in coastal aquifers, Advances in Water Resources, 57, 1-11, doi: 10.1016/j.advwatres.2013.03.011.

Smith, A. J. (2004), Mixed convection and density-dependent seawater circulation in coastal aquifers, Water Resources Research 40, Art. no. W08309, doi: 10.1029/2003WR002977.

Strack, O. D. L. (1976), A single-potential solution for regional interface problems in coastal aquifers, Water Resources Research, 12(6), 1165–1174.

Velstra, J., J. Groen and K. de Jong (2011), Observations of salinity patterns in shallow groundwater and drainage water from agricultural land in the northern part of The Netherlands, Irrigation and Drainage, 60, 51-58, doi: 10.1002/ird.675.

Viezzoli, A., E. Auken and T. Munday (2009), Spatially constrained inversion for quasi 3D modelling of airborne electromagnetic data-an application for environmental assessment in the Lower Murray Region of South Australia, Exploration Geophysics, 40(2), 173–183, doi: 10.1071/EG08027.

Volker, R. E. and K. R. Rushton (1982), An assessment of the importance of some parameters for sea-water intrusion in aquifers and a comparison of dispersive and sharp-interface modelling approaches, Journal of Hydrology, 56(3-4), 239-250, doi: 10.1016/0022-1694(82)90015-4.

Werner, A. D. (2016) On the classification of seawater intrusion, Journal of Hydrology, doi: 10.1016/j.jhydrol.2016.12.012.

Werner, A.D., M. Bakker, V. E. A. Post, A. Vandenbohede, C. Lu, B. Ataie-Ashtiani, C. T. Simmons, D. A. Barry (2013), Seawater intrusion processes, investigation and management: Recent advances and future challenges, Advances in Water Resources 51, 3–26, doi: 10.1016/j.advwatres.2012.03.004.

Werner, A. D., A. Kawachi and T. Laattoe (2016), Plausibility of freshwater lenses adjacent to gaining rivers: Validation by laboratory experimentation, Water Resources Research, 52, doi: 10.1002/2016WR019400.

Werner, A. D. and T. Laattoe (2016), Terrestrial freshwater lenses in stable riverine settings: Occurrence and controlling factors, Water Resource Research, 52, 3654–3662, doi: 10.1002/2015WR018346.

Werner, A. D., J. D. Ward, L. K. Morgan, C. T. Simmons, N. I. Robinson and M. D. Teubner (2012), Vulnerability indicators of sea water intrusion, Ground Water, 50, 48–58, doi: 10.1111/j.1745-6584.2011.00817.x.

Woods, J. (ed.) (2015), Modelling salt dynamics on the River Murray floodplain in South Australia: Conceptual model, data review and salinity risk approaches, Goyder Institute for Water Research Technical Report Series No. 15/9, Adelaide, South Australia. 149 p., www.goyderinstitute.org/uploads/15_9_E.1.11%20Litrev_final%20(1).pdf.